

FEI Electron Optics BV

Field of inserted charges during Scanning Electron Microscopy of non-conducting samples

Taher Amlaki¹, Neil Budko², Eric Bosch³, Nicola Debernardi⁴, Ute Ebert⁵, Vanessa Leung⁶, Martijn Mink⁷, Caterina Prastani⁷, Seyno Sluyterman³, Marieke Snelder¹, Jannis Teunissen⁵, Barend Thijsse², Jos Thijsen²

¹ *University of Twente, the Netherlands*

² *Technical University Delft, the Netherlands*

³ *FEI Company, the Netherlands*

⁴ *Eindhoven University of Technology, the Netherlands*

⁵ *CWI, the Netherlands*

⁶ *University of Amsterdam, the Netherlands*

⁷ *Utrecht University, the Netherlands*

1. Abstract

Three different approaches to calculating the electric potential in an inhomogeneous dielectric next to vacuum due to a charge distribution built up by the electron beam are investigated. An analytical solution for the electric potential cannot be found by means of the image charge method or Fourier analysis, both of which do work for a homogenous dielectric with a planar interface to vacuum. A Born approximation gives a good approach to the real electric potential in a homogenous dielectric up to a relative dielectric constant of 5. With this knowledge the electric potential of an inhomogenous dielectric is calculated. Also the electric field is calculated by means of a particle-mesh method. Some inhomogeneous dielectric configurations are calculated and their bound charges are studied. Such a method can yield accurate calculations of the electric potential and can give quantitative insight in the charging process.

A capacitor model is described to estimate the potential due to the charge build up. It describes the potential build up in the first microseconds of the charging. Thereafter, it seems that more processes have to be taken into account to describe the potential well. This potential can further be used in a macroscopic approach to the collective motion of the electrons described by the Boltzmann transport equations or a derived density model, which can be a feasible alternative approximation to the more commonly used Monte-Carlo simulation of individual trajectories.

2. Company profile

FEI Electron Optics BV, part of FEI Company, develops, produces and sells tools for nanotechnology, focusing on electron microscopy and focused ion beam equipment. Main markets are research institutes and industries in the areas of nano-technology, nano-electronics and nano-biology. Products include TEMs, scanning electron microscopes (SEMs) and equipment with both a FIB and a SEM column (DualBeam). Annual turnover of the company is

around 700M\$. Strategic growth areas include the Life Science market, and soft-materials research.

3. Problem description

In scanning electron microscopy, a primary electron beam is scanning the surface of the sample of interest, using landing energies ranging from 50eV to 30 keV. In response, the sample releases secondary electrons (SEs) and some of the primary electrons are also scattered back (BSEs). At FEI there is an increasing focus on modeling the beam sample interaction, because increased understanding of the images created by the electron microscope is needed to obtain more, reliable information from samples which are often difficult to image. For calculating amounts of SEs and BSEs a sophisticated Monte Carlo program is used. This simulation works well, but difficulties arise when parts of a sample are non-conductive, like in polymers, solar cells or biological samples. Tracking all the holes and electrons that are generated and remain in existence for a significant time makes the calculation of non-conductive samples excessively time consuming.

For this reason we are also looking at different, more macroscopic, semi-analytical models. In this model we need expressions for the field of charged spheres. For the field of a charged sphere in an otherwise uniform space of infinite dimensions the expressions are known and simple, matters get complicated near material boundaries.

In one case, the uniform space is closed at one side by an interface characterized by a change in electrical permeability (ϵ_r) (In an extreme case, this interface can be regarded as a conductive layer). Here we can still find a reasonably simple expression, via the introduction of a so-called 'mirror charge'. So far, it is relatively easy. This is well described in for instance: J.D. Jackson, 'Classical Electrodynamics, second edition', ISBN 0-471-43132-x, section 4.4 (1975).

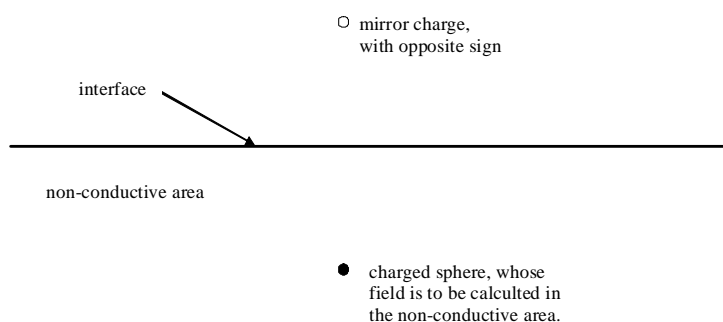


Figure 3.1 Calculating the field of a charged sphere, via the concept of a mirror charge.

The situation becomes more difficult when one also has to deal with interfaces in the horizontal direction, but that is just where the samples get interesting. Then one has to deal with many more mirror charges, as the mirror charges themselves also get mirrored again, as shown in Figure 3.2. This leads to an, in principle unlimited, series of charges. Most likely, this series will converge, but can it also be expressed in a new and simple analytical expression that can be evaluated without consuming too much computation time?

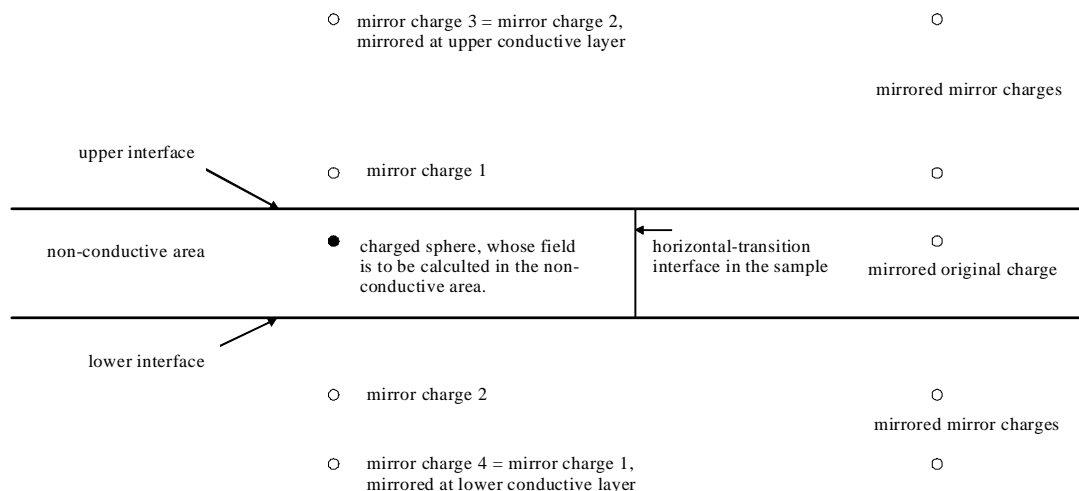


Figure 3.2 Calculating the field of a charged sphere, in case of two parallel horizontal interfaces and a third, perpendicular, interface, via the concept of a mirror charges. Characteristic for the problem is that the mirror charges themselves also get mirrored again.

In conclusion, having easy to use semi-analytical expressions for these cases would be of great help.

4. Problem solving strategy

The problem is split up into two parts. In the first part (chapter 5) we try to calculate the electric potential for an inhomogenous dielectric. In the other part (chapter 6) we concentrate on the influence of the electric field on the diffusion of the electrons in the dielectric and their influence on the electric potential in the dielectric.

For the calculation of the electric potential three different approaches are considered. The first one relies on the Born approximation where the potential generated by the bound charges is considered as a disturbance to the system consisting of the free charges originating from the electron beam in free space. After that the particle-mesh method is considered as a possibility to calculate the electric field in an accurate and fast way. Finally analytical expansion methods are explored.

In chapter 6 we look at two methods to investigate the interaction of the electrons with the potential in the dielectric and their drift and diffusion under influence of this time-varying potential as an alternative to the Monte-Carlo simulations. First of all this is dealt with in a so-called capacitor model. The idea behind this approach is to look at the charging process as a capacitor. In this way quite a simple expression of the potential can be calculated, which can also be used in the macroscopic approach of chapter 6.2. In this approach the collective motion of the electrons is described by the Boltzmann equation which would provide an approximation towards understanding the behavior of the electrons which complements the computationally intensive results obtained by the Monte-Carlo simulations. Another alternative would be a density or hybrid approximation for the electron dynamics.

5. Calculation of the electric potential

This chapter focuses on the calculation of the electric potential caused by the charge implemented by the electron beam and the induced charge due to these electrons in the dielectrics. First the Born approximation is considered in paragraph 5.1 and compared with exact results of the potential of a known configuration. After that, the method is applied to a more com-

plex configuration with different dielectric constant values. In paragraph 5.2 the concept of the particle-mesh method is explained after which the electric potential of a few configurations is calculated and discussed. At last, in paragraph 5.3 an exact analytical solution for the electric potential is searched for by means of a Fourier analysis.

5.1 The Born approximation

Assuming that the dielectric has a linear response to the electric field, the Poisson equation can then be written as:

$$\nabla \cdot (\epsilon \nabla V) = -\rho_f. \quad 5.1.1$$

Here ρ_f is the distribution of charges in the specimen, both the trapped primary charges and the charges induced by the beam. By subtracting $\nabla \epsilon_0 \nabla V$ from both sides we get after some rearrangements:

$$\begin{aligned} \nabla^2 V &= -\frac{\rho_f}{\epsilon_0} - \nabla \cdot \frac{(\epsilon - \epsilon_0) \nabla V}{\epsilon_0}, \\ &= -\frac{\rho_f}{\epsilon_0} - \nabla \cdot (X \nabla V), \\ &\text{where } X = \frac{\epsilon(r) - \epsilon_0}{\epsilon_0}. \end{aligned} \quad 5.1.2$$

Then we split the potential into two parts; one caused by the 'free charge', which is the same charge distribution as above but taken in vacuum, and one caused by the 'bound charge', which is the remaining correction term due to the dielectric. That is:

$$V = V^{free} + V^{bound}, \quad 5.1.3$$

and

$$\nabla^2 V^{free} = -\frac{1}{\epsilon_0} \rho_f. \quad 5.1.4$$

Comparing this expression with the equations written above, we can write the potential caused by the bound charge as:

$$\nabla^2 V^{bound} = -\nabla \cdot (X \nabla V) \quad 5.1.5$$

We know how to solve the potential for the free charge as that is the charge that comes from the electron beam in a homogenous medium. Formally, we can solve the potential for the bound charge in exactly the same way:

$$V^{bound}(r) = \int \frac{1}{4\pi|r-r'|} \nabla' \cdot (X(r') \nabla V(r')) dr'. \quad 5.1.6$$

In the Born approximation it is assumed that the potential caused by the bound charge is small so that the potential in the integral can be replaced by V^{free} . Then everything in the integral is known and the potential of the bound charge can be estimated in this way. If the estimation is not accurate enough one can substitute a new potential in the integral of equation 5.1.6: $V = V^{free} + V^{bound}$ where V^{bound} is the potential calculated from substituting V^{free} in the integral of equation 5.1.6. This can be continued till the series is converging.

Remark: It might be worthwhile to reverse the procedure, namely to calculate the unperturbed solution in the dielectric rather than in the vacuum and to take the vacuum as a perturbation, but this has not been tried in the course of the week.

5.1.1 Comparison of different dielectric values

To evaluate the usefulness of the Born approximation, we first focus on one single interface as depicted in Figure 1. because for this configuration exact solutions already exist. This makes it easier to compare and evaluate its validity.

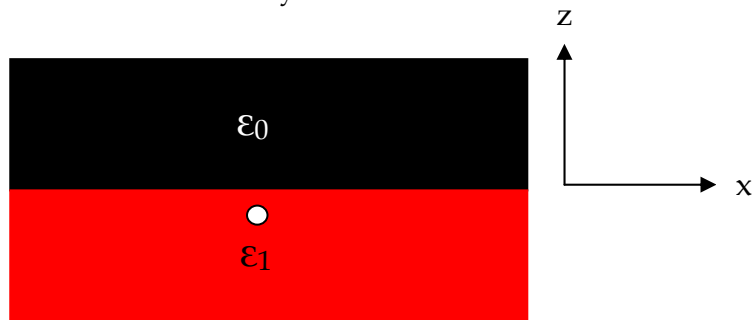


Figure 5.1 The used configuration to investigate the usefulness of the Born approximation

A point charge is set in the dielectric with permittivity ϵ_1 at coordinates $(0, 0, -1)$ (the white point in Figure 5.1). Here the origin is taken at the midpoint of the configuration. The permittivities are taken relative to the vacuum. With *Mathematica* the electric potential is calculated for the exact solution obtained through the image charge method, for the electric potential with the point charge in free space and for the electric potential calculated by means of the Born approximation. By plotting the potential in vacuum it is seen that the potential is almost zero at the points -5 and 5 in all directions. Integrating in a larger domain is only noticeable in the third decimal of the value of the potential on a certain place. Therefore the integration is from -5 till 5 in all directions. In Figure 5.2 two plots are shown in which we plot the potential as a function of the z coordinate following the line $(1,0,z)$. The left plot corresponds to a permittivity $\epsilon_1 = 1.5$ (where here and elsewhere we take $\epsilon_0 = 1$), while the right plot corresponds to $\epsilon_1 = 5$. The top (dashed) line shows the exact solution, the middle (solid) line the result of the Born approximation, and the bottom (dotted) line the zeroth order result, in which the dielectric boundary is neglected. We see that for $\epsilon_1 = 1.5$ it is a very good approximation to the exact result. For higher value $\epsilon_1 = 5$, the difference with the exact solution increases, but still the Born approximation gives a much better result than the zeroth order curve.

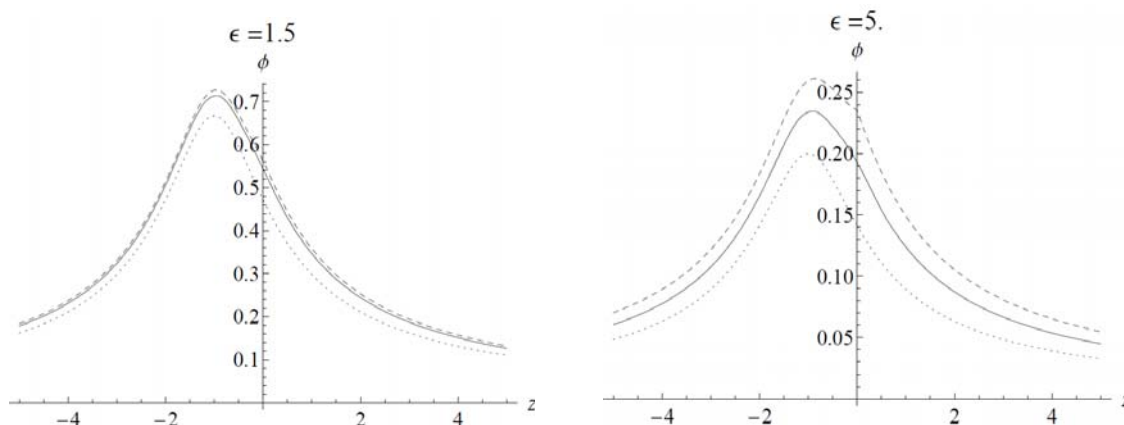


Figure 5.2 The potential in the dielectric setup Figure 5.1 as a function of the z coordinate following the line $(1,0,z)$. The left plot corresponds to a permittivity $\epsilon_1 = 1.5$, the right plot to $\epsilon_1 = 5$. The top (dashed) line shows the exact solution, the middle (solid) line the result of the Born approximation, and the bottom (dotted) line the zeroth order result, in which the dielectric boundary is neglected.

Next, we consider the dielectric setup shown in Figure 5.3. An extra dielectric interface is added in the lower region and the point charge is located at $(0,0,-1)$ to the left of it.



Figure 5.3 The dielectric setup with an extra dielectric interface.

In Figure 5.4 two plots are shown in which we plot the potential as a function of the z coordinate following the line $(0,0,z)$. The left plot corresponds to a permittivity $\epsilon_1 = 1.5$ and $\epsilon_2 = 2$, while the right plot corresponds to a $\epsilon_1 = 1.5$ and $\epsilon_2 = 6.5$. The bottom solid line shows the result of the Born approximation for this system. The top (dotted) line shows the potential of the dielectric setup of Figure 5.1, with $\epsilon_1 = \epsilon_2 = 1.5$ for comparison. We see that the potential is decreasing for a higher ϵ_2 value, which is caused by the induced negative charge at the extra interface between regions 1 and 2. Thus, we see that also for this system, the results of the Born approximation are very reasonable.

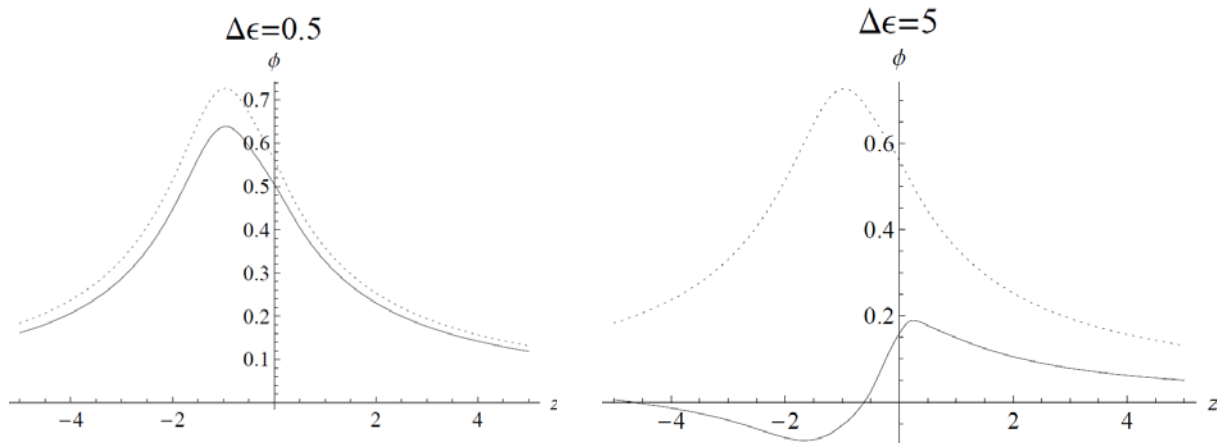


Figure 5.4 The potential as a function of the z coordinate following the line $(1,0,z)$. The left plot corresponds to a permittivity of $\epsilon_1=1.5$ and $\epsilon_2=2$, while the right plot corresponds to $\epsilon_1=1.5$ and $\epsilon_2=6.5$. The bottom solid line shows the result of the Born approximation for this system. The top (dotted) line shows the potential of the dielectric setup of figure 5.1, with $\epsilon_1= \epsilon_2=1.5$ for comparison.

5.2 Numerical methods for the computation of the electric field

There are many numerical methods to obtain the electric field (or equivalently, the electric potential) of a given charge configuration. If the charges are represented as particles, the most direct methods sum the contributions of the individual particles to obtain the electric field at some point. It should be clear that such an approach becomes very expensive when the number of particles increases, and they should mostly be used when close range interactions need to be resolved accurately.

An alternative to the direct methods is to use a particle-mesh or particle-in-cell (PIC) method. With such a method one first maps the particles to charge densities on a mesh, after which

the electric potential is computed (given some boundary condition) and from that the electric field. Particles can still be simulated individually, but they now move in a field computed from the charge density. Interactions over a distance comparable to the mesh spacing might not be resolved accurately in this way, but for many applications these do not contribute significantly to the overall behavior. If close range interactions are important one can work with a P³M method, which combines the particle-particle interaction at close range with a particle-mesh method.

5.2.1 Particle-mesh method

To simulate the charging of samples due to the scanning electron beam, we suggest a particle-mesh method, as the number of charged particles in the samples will typically be quite large and close range interactions seem not to be crucial for the charging process, except for detailed trajectories of single particles. Depending on the required accuracy one first has to choose a type of mesh. Then the Poisson equation can be solved on this mesh with some boundary condition, and the electric field is obtained by taking the numerical gradient. For a practical simulation it would probably be best to recompute the electric field only after N electrons have landed from the beam, where N is chosen such that the beam deposits a significant amount of charge in this interval.

There are many algorithms available to compute the potential, and the choice of algorithm typically depends on the type of mesh used and the boundary conditions, see for example chapter 6 of 'Computer Simulation Using Particles' by R.W. Hockney and J.W. Eastwood [1]. If the domain contains materials with different dielectric constants or has a non-rectangular geometry the so-called fast solvers (based on cyclic reduction and the fast Fourier transform) can usually not be used. Methods based on mesh relaxation are more flexible in this regard, as are finite element methods. When one wants to simulate the charging of the sample together with the beam interaction, performance is essential. We therefore suggest that a multigrid method with adaptive grid refinement and special treatment of the dielectric interfaces could be used, see for example Deng et al. [2]. They also describe a different method for the case where all the dielectrics are rectangular, which uses a fast solver on the rectangular subdomains and an iterative procedure to match the boundary conditions between the subdomains.

Although there is a lot of literature on algorithms for solving the Poisson equation, there seem to be no codes available that fulfil all the requirements described above. The development of such codes is far from trivial, and therefore we have developed a simple relaxation method during the week, to demonstrate the principles and also get some physical insight. We started out with successive over-relaxation on 2D and 3D Cartesian grids and a Dirichlet boundary condition. See Figure 5.5a for an example of the computed potential in 2D. It can clearly be seen that the positive charge induces a negative surface charge on the dielectric, see Figure 5.5b where we show the polarization charge for a different configuration.

The change in dielectric constant cannot be more than about a order of magnitude, or else the iteration becomes unstable. We have also worked with a simple multigrid algorithm, in which we saw that the rate of convergence depends on the location of the dielectric boundary. This illustrates that special treatment of the interfaces is required to have a fast and stable method.

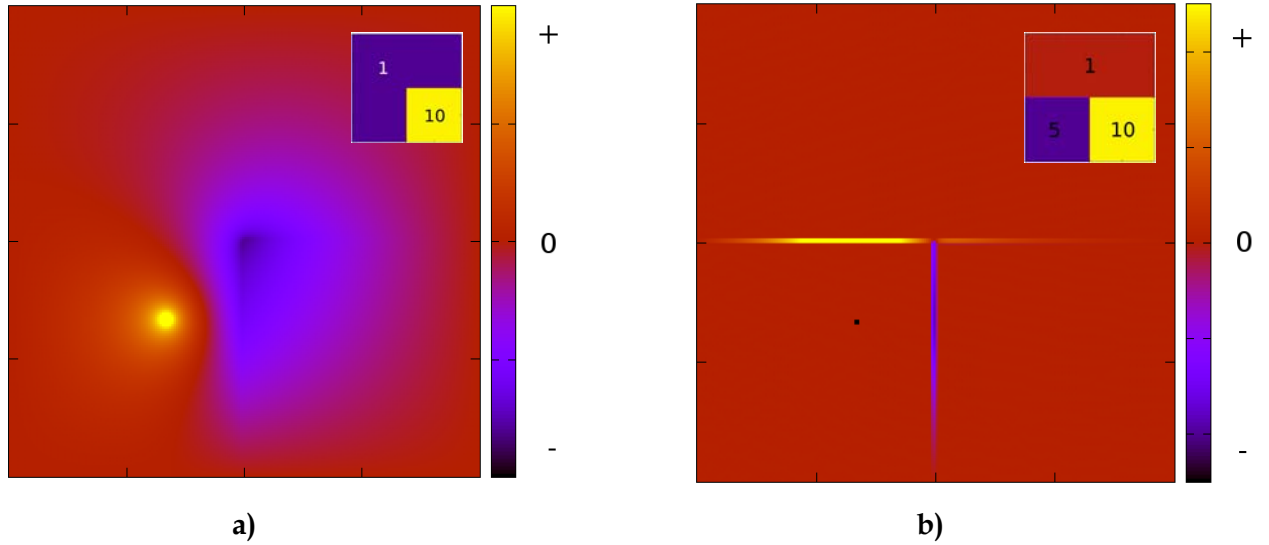


Figure 5.5 a) The potential due to a positive point charge in vacuum next to a dielectric (at the same location as the black dot in b)). The relative dielectric constants are shown in the top right. Clearly the positive charge induces a negative polarization charge on the dielectric interface, which significantly lowers the potential in a large part of the domain. The boundary was grounded in this calculation. b) The polarization charge density induced by a positive point charge (the black dot). It can be seen that the sign of the induced polarization charge depends on whether the dielectric constant increases or decreases along an interface.

5.3 Analytical solution to Poisson equation

One classical way to solve Poisson equation is to expand the potential by using a complete set of functions as a basis and finding the appropriate coefficients which satisfy the boundary conditions. We decided to use a continuous basis in the Cartesian representation and therefore we wrote the potential in three different parts like this:

$$\Psi_{1(3)} = \iint dk_x dk_y e^{i(k_x x + k_y y)} e^{-k|z|} A_{1(3)}(k_x) B_{1(3)}(k_y) \quad 5.3.1$$

$$\Psi_2 = \Phi_p + \iint dk_x dk_y e^{i(k_x x + k_y y)} e^{-k|z|} A_2(k_x) B_2(k_y) \quad 5.3.2$$

where Φ_p is the potential of the point charge. Here the configuration and the coordinate axes are the same as in Figure 5.3 but the three dielectric regions are numbered 1, 2, 3 instead of 0, 1, 2.

We have three boundaries and six boundary conditions, which are:

$$\Psi_1(x > 0, y, z = 0) = \Psi_3(x > 0, y, z = 0) \quad 5.3.3$$

$$\Psi_1(x < 0, y, z = 0) = \Psi_2(x < 0, y, z = 0) \quad 5.3.4$$

$$\Psi_2(x = 0, y, z) = \Psi_3(x = 0, y, z) \quad 5.3.5$$

$$\left(\varepsilon_1 \frac{\partial \Psi_1(x > 0, y, z^+)}{\partial z} + \varepsilon_3 \frac{\partial \Psi_3(x > 0, y, z^-)}{\partial z} \right)_{z=0} = 0 \quad 5.3.6$$

$$\left(\varepsilon_1 \frac{\partial \Psi_1(x < 0, y, z^+)}{\partial z} + \varepsilon_2 \frac{\partial \Psi_2(x < 0, y, z^-)}{\partial z} \right)_{z=0} - \varepsilon_2 \frac{\partial \Phi_p}{\partial z} \Big|_{z=0} = 0 \quad 5.3.7$$

$$\left(\varepsilon_2 \frac{\partial \Psi_2(\mathbf{x}^-, y, \mathbf{z})}{\partial \mathbf{x}} + \varepsilon_3 \frac{\partial \Psi_3(\mathbf{x}^+, y, \mathbf{z})}{\partial \mathbf{x}} \right)_{x=0} + \varepsilon_2 \frac{\partial \Phi_P}{\partial \mathbf{x}} \Big|_{x=0} = 0 \quad 5.3.8$$

by using the equations for the boundary between regions 2 and 3 we could derive this relation:

$$B_2(k_y)(A_2(k_x) + A_2(-k_x)) = \frac{\varepsilon_3 f_o + f_1}{\varepsilon_2 + 1} \quad 5.3.9$$

$$B_3(k_y)(A_3(k_x) + A_3(-k_x)) = \frac{f_1 - \varepsilon_2 f_o}{\varepsilon_3 + 1} \quad 5.3.10$$

where f_o, f_1 are related to the Fourier transformations of the Bessel function by:

$$f_o = \int dy e^{-iky} \frac{q}{\varepsilon_2} J_o(k\rho) \quad 5.3.11$$

$$f_1 = x_o \int dy e^{-iky} \frac{q}{\varepsilon_2} \frac{k J_1(k\rho) e^{kz_o}}{\rho} \quad 5.3.12$$

and

$$\rho = \sqrt{x_o^2 + (y - y_o)^2 + z_o^2} \quad 5.3.13$$

$$k = \sqrt{k_x^2 + k_y^2} \quad 5.3.14$$

The next step is to use these relations in the boundaries between 1,2 and 1,3, but because at the boundary of 1,2 x is negative and in 1,3 it is positive, we cannot take the inverse Fourier transformation and also we could not eliminate A_1, B_1 from the equation, so we could not solve the problem analytically. We also tried some other expansions by using an infinite and countable basis, but they also failed.

6. Potential development due to charging and electron motion in a dielectric

This chapter deals with the development of the potential due to charging and the motion of the electrons in the dielectric itself. In the first paragraph a capacitor model is discussed which deals with the charge distribution as a spherical capacitor. Next, the collective motion of the electrons is discussed by means of a Boltzmann equation which has the potential to lead to an alternative method for calculating their distribution to the Monte Carlo simulations usually encountered in literature. Another alternative would be a density model derived from moments of the Boltzmann equation.

6.1 Capacitor model

The energy of the primary beam influences the range of the electrons in the medium as follows:

$$R(E_{PE}) = \frac{\beta}{\rho} \left(\frac{E_{PE}}{1eV} \right)^{1.65}, \quad 6.1.1$$

where, for silicon, $\beta=0.76 \times 10^{-9} \text{ kg/m}^2$ and $\rho=2330 \text{ kg/m}^3$. The range for electrons with $E_{PE}=15 \text{ keV}$ in Si is therefore about $2.5 \mu\text{m}$.

The yield of the secondary electrons also depends on the primary beam energy as

$$\delta(E_{PE}) = \frac{0.5}{\xi} \frac{E_{PE}}{R(E_{PE})} \lambda (1 - e^{-R(E_{PE})/\lambda}), \quad 6.1.2$$

where $\xi=90$ [eV/escaped SE] and $\lambda=2.7 \times 10^{-9}$ [m]. This is calculated to be 0.006 for the case of Si and an energy $E_{PE}=15$ keV. The yield of the back-scattered electrons is a constant, $\eta=0.2$.

6.1.1 Capacitor model for a single pixel

At a fixed beam position, the positive charge is created mainly below the surface at about 17 nm. The positive charge originates from the fact that the generated secondary electrons leave the sample. The primary electrons drift and diffuse into the sample over a mean distance R and tend to become deposited in a half circular shape at a distance R under the surface. The typical sample thickness d is 200 μm . This situation is schematized in the following Figure:

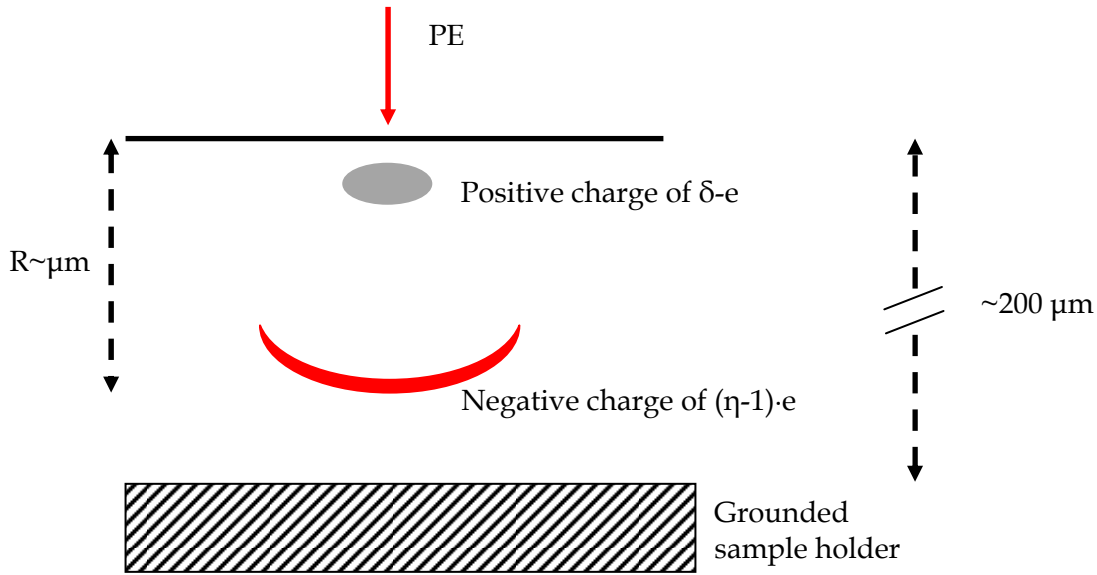


Figure 6.1 Sketch of the charge build up in a dielectric on a sample holder exposed to an electron beam due to the electrons originated from the beam.

Since R is so much smaller than d , it is safe to say that all charge is deposited at a distance d from the sample holder, which is at ground potential. Even if the configuration look like a dipole, it is interesting to approximate the geometry as the charge has been deposited in a spherical shape. Under those circumstances the charged area (also called the interaction volume) can be seen as a spherical capacitor at a distance d from a grounded wall, at the bottom of the sample.

The capacitance of a sphere with a radius $r=R/2$ is given by the following formula, where $D=d/r$ [3] :

$$C_s = 4\pi r \epsilon_0 \epsilon_r \sum_{n=1}^{\infty} \frac{\sinh(\ln(D + \sqrt{D^2 - 1}))}{\sinh(n \ln(D + \sqrt{D^2 - 1}))}. \quad 6.1.3$$

The series converge well, if truncated after $n=3$, to $C_w \approx 1.7 \cdot 10^{-15}$ F, for the dielectric constant of silicon ($\epsilon_r=11.9$).

The voltage in a capacitor follows this relation [3]

$$V(t) = \frac{Q(t)}{C}, \quad 6.1.4$$

where V is the voltage, C the capacitance and Q the charge. The time-dependent charge can be written as: [3]

$$Q(t) = I(1 - \eta - \delta)t, \quad 6.1.5$$

with I the intensity of the beam and t the dwell time. This charge Q is the net negative charge in the sample. The following Figure shows a plot of the voltage versus the dwell time, for the case of a spherical capacitor with a beam current of 1 nA.

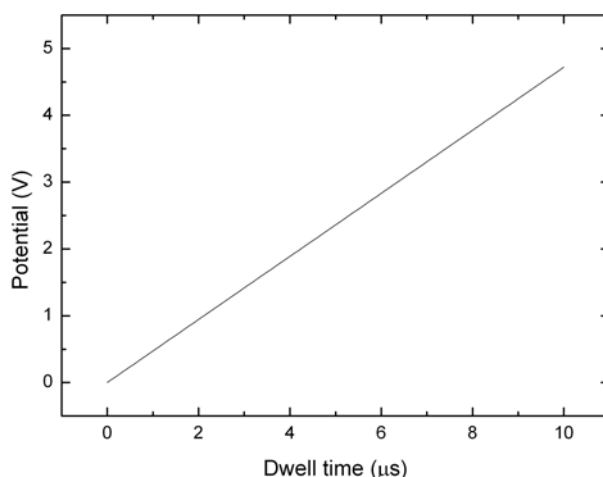


Figure 6.2 Voltage versus dwell time for a spherical capacitor with a beam current of 1 nA calculated with the help of formulas 6.1.5 and 6.1.6 for the case of Si. The voltage is negative.

This exercise can show that in a typical dwell time a potential of 5 V can build up in a typical measuring point (one pixel). This potential can influence the trajectory of secondary electrons of few eV energy.

This voltage decays in time, similarly to a RC circuit. But in order to get the time constant $\tau = R \cdot C$, it is necessary to find an expression of the resistance, which is missing at the moment.

6.1.2 Capacitor model for a line scan

A typical SEM scan pattern is made up of 1000 by 1000 pixels. Every pixel is illuminated with for instance 1 nA beam current for 1 to 10 μs . In general, a pixel is influenced by the electric field of the previous illuminated ones. It is interesting to approximate a line scan as the charge is deposited as a wire configuration. The capacitance of a wire with a length $l = 1 \mu\text{m}$, put at a distance $d = 200 \mu\text{m}$ from the wall is given by [3]

$$C_w = \frac{2\pi l \epsilon_0 \epsilon_r}{\ln(D + \sqrt{D^2 - 1})} \quad 6.1.6$$

and with this geometry it results in $C_w \approx 1.0 \cdot 10^{-16}$ F.

But in order to evaluate the potential, it is necessary to know the how fast the potential decays in each pixel with respect the scanning time.

6.1.3 Yield vs. Energy

The total yield of BSE and SE depends on the energy of the primary electron beam as in Figure 6.3.

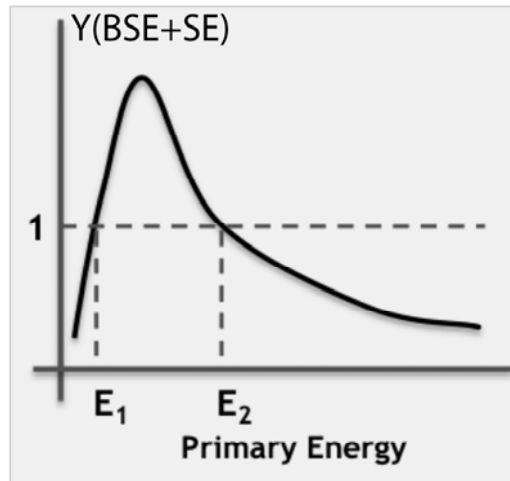


Figure 6.3 Schematic graph of the sum of the back-scattered electrons (BSE) and the secondary electrons (SE) as a function of the energy of the incident electrons on a sample. The vertical axis displays the total yield $Y(\text{BSE}+\text{SE}) = \eta + \delta$.

For a beam energy greater than E_2 , the sample accumulates a negative charge since the net yield is less than one. With time, the negative charge accumulated below the surface of the sample slows down the primary beam towards an energy E_2 . At this point, the yield equals 1, so there is not a net change of the charge in the sample. On the other end, with a primary beam energy smaller than E_2 (but larger than the maximum of the function), the samples charge up positively, since for every landing electron, there is more than one electron leaving the sample per landing event. This positive potential tends to attract back the secondary electrons and they gradually do not leave the sample. The points with an energy E_2 is a stable points.

From SEM pictures, the charging process appears to stabilize after a certain time (a scan of few seconds at a MHz measuring rate per pixel), meaning that the net charge is not changing. From the results presented here, the potential increases with time. But this is not in contrast with the measurements, because in the experiments, even when the net charge seems to be constant, there is an ongoing change in charge *distribution* leading to internal electric

6.2 Electron Transport – a possible alternative to Monte-Carlo simulations

The Monte-Carlo method of simulating the dynamic charge distribution of electrons in a dielectric sample by tracing numerous trajectories is powerful and versatile but also computationally intensive. It is therefore interesting to look for possible alternatives to this approach.

One strategy which suggests itself is a model based on the drift and diffusion of electrons in the medium. Instead of concentrating on the motion of individual particles, the collective behavior of all the particles can be modelled as the dynamic evolution of an out-of-equilibrium system relaxing to its steady state. We start with a very high concentration of electrons at the surface of the dielectric, which then spread through the bulk of the material to some final position and momentum distribution. In the primary beam, of course, all electrons start with a common high entrance velocity at their initial positions at the surface.

Some questions immediately arise. For example, can the motion of such high energetic particles really be modelled as a Brownian diffusion process? And how would one describe in such a model the deceleration of the particles as they are slowed down by inelastic collisions?

The dynamic evolution of an ensemble of particles towards equilibrium is described by the Boltzmann Transport equation:

$$\frac{\partial f}{\partial t} = \left(\frac{\partial f}{\partial t} \right)_{force} + \left(\frac{\partial f}{\partial t} \right)_{diff} + \left(\frac{\partial f}{\partial t} \right)_{coll} \quad 6.2.1$$

where $(\partial f / \partial t)$ is the particle distribution function, which depends on the velocity v , position r , and time t . $(\partial f / \partial t)_{force}$ is the rate of change of the external driving force, in this case an electric field, $(\partial f / \partial t)_{diff}$ is the rate of diffusion, and $(\partial f / \partial t)_{coll}$ is the collisional rate.

From this general view of transport, the challenge is to find appropriate models based on the Boltzmann equation, specific to the distribution of charges in scanning electron microscopy. The strategy we propose is to divide the electron population which plays a role in the charge build-up process into two categories, based on their energies.

Secondary electrons, or other electrons with energies less than 5 eV (that do not create additional free particles), can be well-described by the Boltzmann transport equation normally used for modeling, for example, the flow of electrons in silicon or other semi-conductor material. Analytical solutions as well as approximations have been demonstrated, which allow the calculation of parameters such as the electron energy distribution and electron drift velocities [4, 5]. The results from these models can be shown to compare favorably to Monte-Carlo simulations [5].

Primary and back-scattered electrons with energies of greater than 100 eV require an additional approximation, in order to adequately describe the deceleration of these high-energy particles through inelastic scattering processes. The Continuous Slowing-Down Approximation (CSDA) allows the net distance an electron travels in various media to be estimated by assuming that the energy of the electron decreases at a constant rate. Materials for which the CSDA range is known include, for example, silicon and polystyrene [6].

By combining the Boltzmann Transport Equation with CSDA, we come upon an electron transport model known as the Spencer-Lewis equation. This equation is used mainly in nuclear and particle physics, where it was important to understand, for example, the behavior of a high-energy electron impacting on a silicon detector. Three-dimensional numerical solutions of this equation have been calculated for electrons in silicon in various geometries, where it is also claimed that good agreement with Monte-Carlo results have been achieved with this method and that it is significantly faster [7].

This investigation shows therefore that there are indeed precedents for an alternative approach, one which tries to understand the problem presented through an electron transport model. If it proves feasible on a practical level, such an approach may allow gains in computational time, as well as provide a deterministic calculation method which permits the change of one parameter while keeping every other characteristic of the system identical. For some applications these advantages could complement well with Monte-Carlo simulations.

Finally, we should mention that other 'global' approaches besides the electron transport equation also exists, such as the Fokker-Planck equation, and even with the electron transport approach there are many different variants, for example self-consistency [8].

Another alternative lies in deriving an electron density approximation by averaging over moments of the Boltzmann equation. This might yield a better approximation of the collisional processes and successive reaction products (like excitations and additional free particles) for the energetic particles than the CSDA. (This statement is certainly valid in a gas discharge and needs to be checked in a discharge in a dielectric.) Another approximation consists of treating the energetic particles with a Monte-Carlo approach and the low energy

electrons as densities in a so-called hybrid scheme. The methods mentioned in this paragraph have been developed for collision dominated plasmas in gases.

7. Discussion

Both the Born approximation and the particle-mesh method are useful methods to calculate the electric potential in an inhomogeneous dielectric. One can also go beyond the Born approximation where the calculated corrected potential is used as an input for computing the following higher order correction to the electric potential until the potential converges. However, one should remember that the convergence behaviour of such an iterative series is not checked when one starts from the potential of a homogeneous dielectric. To be sure that the series is converging, the first guess of the potential should be reasonably good. This can be done by simulating different configurations to get a feeling for where the bound charges are located and therefore can help to make a first estimate of the potential of a more complicated dielectric. These simulations can for example be done with the particle-mesh methods with which the computation of the electric field of the charging sample can be probably be done accurately and fast enough to provide some quantitative insight to the charging process. Such a particle-mesh or particle-in-cell method can also be used directly if the particle nature of the electrons does not need to be accounted for. However, the development of such a code will take considerable time and could not be accomplished in the course of the week.

An analytical method for point charges was considered as well, but we stated that an exact analytical solution for an electric potential in an inhomogeneous dielectric next to vacuum cannot be found.

The capacitor model can probably estimate the potential built up due to charging in the very beginning of the charging process. Although the continuous increase of the potential is not in contrast with the stabilization of the charging, it is most likely that other processes have to be taken into account after a few microseconds to explain the behavior of the charge build up in the dielectric that simplify by the separation of the positive and the negative charges. Electron transport models can be used as a complement to Monte-Carlo simulations, providing a global statistical view of the distribution of electrons as they move through the bulk of the dielectric. Precedents exist from solid-state, nuclear, particle and plasma physics, and these can be used as a basis for modeling the current problem, covering the behavior of electrons as both low and high energies.

8. References

- [1] R.W. Hockney and J.W. Eastwood. *Computer Simulation Using Particles*. Taylor & Francis, January 1989.
- [2] S. Deng, K. Ito, and Z. Li. 2003. Three-dimensional elliptic solvers for interface problems and applications. *J. Comput. Phys.* **184**, 1 (January 2003), 215-243.
- [3] J.D. Jackson, (1975). *Classical Electrodynamics*. Wiley.
- [4] L.R. Logan, H.H.K. Tang, and G.R. Srinivasan, *Analytic solutions to the Boltzmann equation for electron transport in silicon*, *Physical Review B* **43**, 6581 (1991).
- [5] O. Muscato, *Relaxation-time approximations to the Boltzmann equation for electron transport in bulk silicon*, *Physica A* **317**, 113 (2003).
- [6] Lawrence Berkeley National Laboratory, *X-ray Data Booklet*, <http://xdb.lbl.gov/> (2009).
- [7] W.L. Filippone, S.P. Monahan, S. Woolf, and J.C. Garth, *Three-Dimensional Multiregion Sn Solutions of the Spencer-Lewis ElectronTransport Equation*, *Nuclear science and engineering* **105**, 52 (1990).

- [8] S.P. Singh, N. Goldsman, I.D. Mayergoyz, *Modeling multi-band effects of hot electron transport in silicon by self-consistent solution of the Boltzmann transport and Poisson equations*, *Solid-State Electronics* **39**, 1695 (1996).